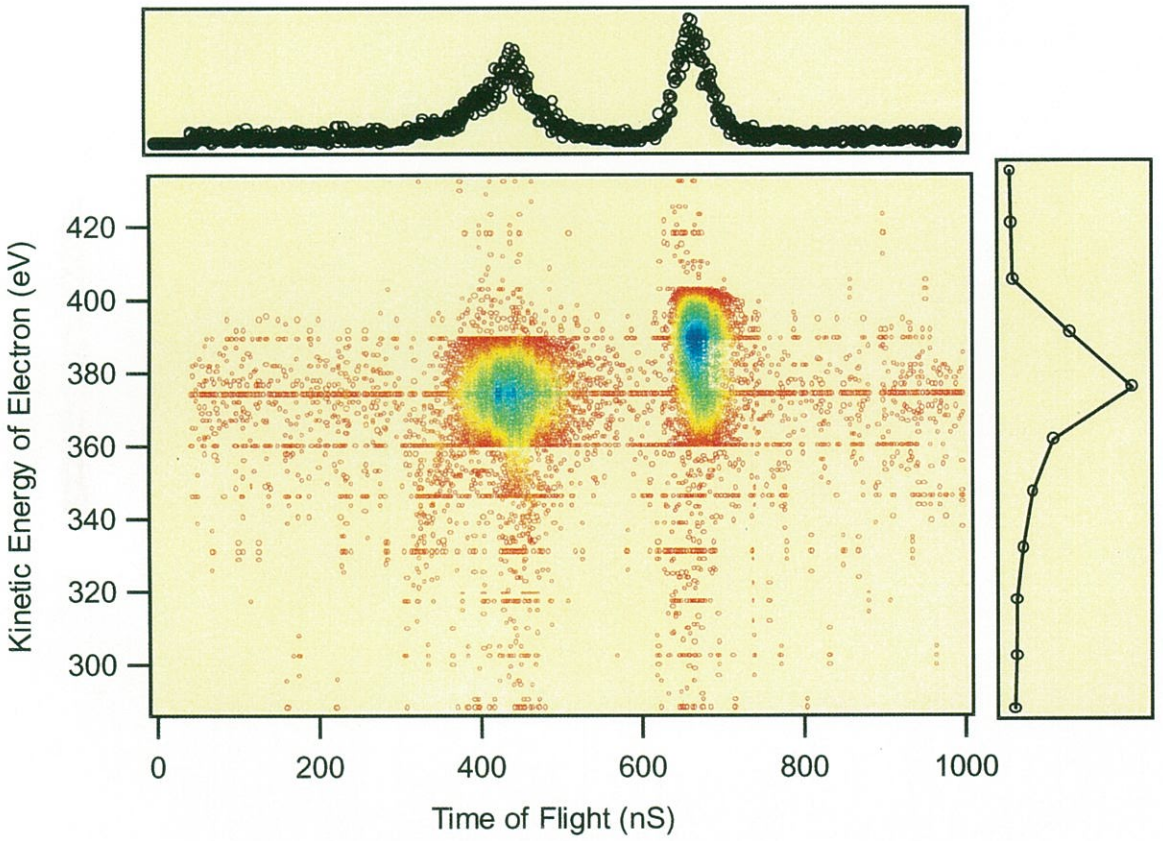

Gas-phase Spectroscopy

BL2B2, 3A2, 3B, 8B1

(BL3A2)

Two-dimensional imaging technique for measuring translational energy and angular distribution of ionic photofragments

Tatsuo Gejo, Eiken Nakamura, Eiji Shigemasa and Norio Saito [A]

Institute for Molecular Science, Myodaiji, Okazaki 444-8585, Japan

[A] *Electrotechnical Laboratory, Umezono, Tsukuba-shi, 305-0045, Japan*

During the last decade, the dynamics of molecules in the valence energy regime has been investigated by preparing excited state at well-defined energy, and analyzing photoelectron energy and angular distribution of ionic photofragments involved. Two-dimensional (2D) imaging technique is one of the most powerful tools for obtaining this information because 2D data and its simple calculation on the basis of momentum conservation law, provide Newton diagram of photofragments, which leads to dynamical process involved immediately

At beamline 3A2 of UVSOR, we have tested this two-dimensional imaging system using a position sensitive detector (PSD) (Roendek). Last year, although, we successfully measured the image of N^+ and N_2^+ signals from nitrogen molecules in the valence excitation region (20-100 eV), significant noise level excluded us from analyzing data. Therefore, we have improved mechanics and electronics as follows:

1) Molecular beam was replaced with an effusive beam from a nozzle.
2) The flight region of photofragments was made shorter.
3) A new TDC system (Lecry4208) was introduced, allowing us to develop our software system.

The system mainly consists of accelerator lens, a PSD and an electronic system for data analysis and a computer. After the gas passes synchrotron radiation (SR) region, less than one molecule per one photon beam on the average undergoes ionization and/or dissociation. The direction of polarization of SR is parallel to the axis of TOF tube (10 cm). After the acceleration by the ion lens, ionic fragments fly through the TOF tube and hit the PSD. The determination of the impact position on the detector is based on the time delay between two signals from each end of a the wire behind the MCP. The position is obtained by the subtracting of time when each two signals arrive, providing us its velocity and direction in the center-of-mass frame. Fig. 1 shows the 2D imaging of N_2^+ after the excitation of the valence electrons. This figure indicates that the interaction region was relatively large because the photon beam was not well focused.

With this technique, we will try to perform the triple coincidence in the ionic fragmentation following inner-shell excitation.

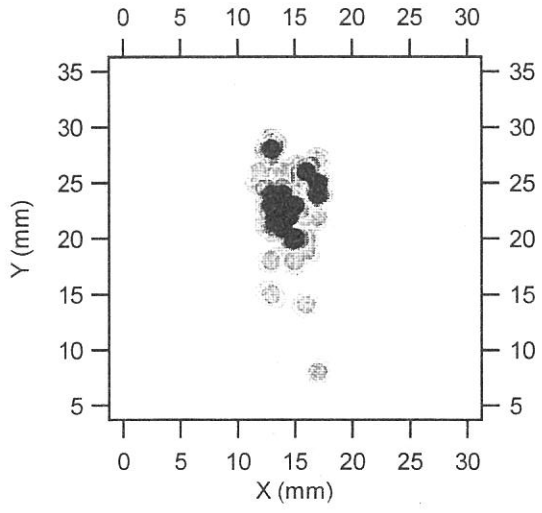

Fig. 1: 2D imaging from N_2^+.

(BL3A2)

Single- and double-photoionization of nitrogen dioxide (NO_2) and ionic fragmentation of NO_2^+ and NO_2^{2+}

Toshio MASUOKA

Department of Applied Physics, Faculty of Engineering,, Osaka City University, Sugimoto 3, Sumiyoshi-ku, Osaka 558-8585

Doubly charged molecular ions are produced in abundance at high energies. However, since molecular double ionization (m^{2+}) is usually followed by the production of an ion pair ($m_1^+ + m_2^+$, dissociative double ionization) doubly charged molecular ions are rare or non-existent in the mass spectra of many molecules. In the determination of double-photoionization cross section (σ^{2+}), it is essential to include both the stable m^{2+} ions (if they exist) and the $m_1^+ + m_2^+$ ion pairs. Another problem is that the m_1^+ ion is produced from m^+ or m^{2+} at excitation energies where dissociative single and double photoionization take place concomitantly. It is desirable to determine how many m_1^+ ions are produced respectively from m^+ and m^{2+}.

In the present study, molecular and dissociative single- and double-photoionization processes of nitrogen dioxide are examined in the photon energy region of 37-120 eV by use of time-of-flight mass spectrometry and the photoion-photoion-coincidence method together with synchrotron radiation. The TOF mass spectra and the PIPICO spectra were measured at an angle of ~55° with respect to the polarization vector where the second-order Legendre polynomial is close to zero. Under these conditions, the effects of anisotropic angular distributions of fragment ions are minimized [1].

Shown in Fig. 1 is a typical time-of-flight mass spectrum measured at a photon energy of 100 eV by using the rf frequency as the start input of a TAC under the single bunch mode. The spectrum is complicated because two or three bunches pass the front end of the beam line in the time range of the mass spectrum. The ratio of double to single photoionization is shown in Fig. 2. Above 100 eV, the ratio exceeds 0.2. This ratio may be regarded as a lower limit of σ^{2+}/σ^+ because the O^++O^++N channel of NO_2^{2+} is not included in the evaluation of σ^{2+} and discrimination effects against energetic ions produced in dissociative double photoionization has not been corrected. However, it should be noted that the correction due to the latter effects is at most about 10% since the average kinetic energy release is about 10 eV at 100 eV for the N^++O^+ dissociation channel and about 7 eV for the O^++NO^+ channel [2]. Since the total photoabsorption cross section of NO_2 in this photon energy region has been reported by Au and Brion [3], the σ^{2+}/σ^+ ratio can be converted to the absolute cross sections for the single and double photoionization.

Ion branching ratios for the individual ions respectively produced from the parent NO_2^+ and NO_2^{2+} ions are determined separately, thus enabling more detailed study of the dissociation processes of the NO_2^+ and NO_2^{2+} ions. These results are shown in Figs. 3 and 4. Looking at the ion branching ratios of NO_2^+, we notice that there is no outstanding variation in the fragmentation as a function of photon energy. Only the O^+ ion increases with photon energy. The thresholds for the O^++NO^+ and N^++O^++O dissociation channels of NO_2^{2+} are at 34.7±0.5 and 43.6±0.2 eV, respectively. These thresholds observed in the present study are in good accordance with those reported previously [4]. The O^++NO^+ dissociation channel of NO_2^{2+} is dominant below 90 eV and above this energy the N^++O^++O channel is a main dissociation process. Charge localized dissociation products, N^{2+} and O^{2+}, are observed above 60 eV.

REFERENCES

[1] T. Masuoka, I. Koyano, and N. Saito, J. Chem. Phys. **97**, 2392 (1992).

[2] T. Masuoka, unpublished data.

[3] J. W. Au and C. E. Brion, Chem. Phys. **218**, 109 (1997).

[4] P. G. Fournier *et al.*, J. Chem. Phys. **89**, 3553 (1988); J. H. D. Eland, Mol. Phys. **61**, 725 (1987).

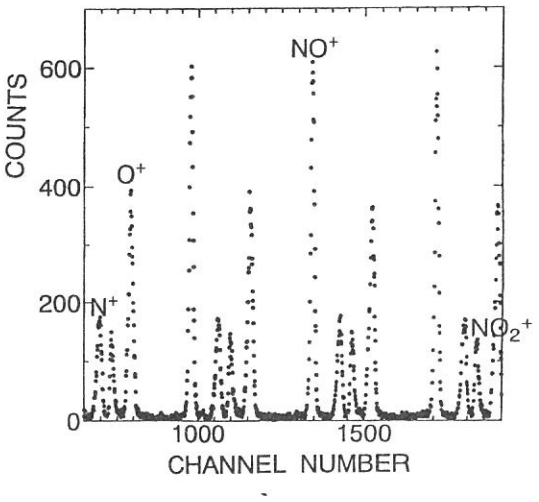

FIG. 1. A typical time-of-flight mass spectrum measured at a photon energy of 100 eV by using the rf frequency as the start input of a TAC under the single bunch mode operation.

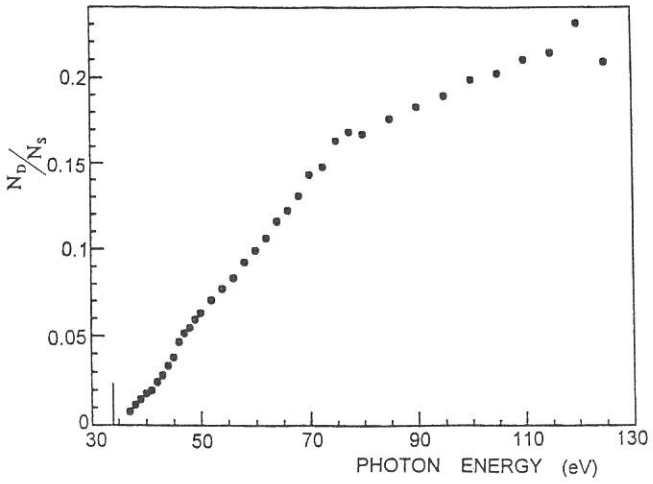

FIG. 2. Ratios of double to single photoionization cross section of NO_2.

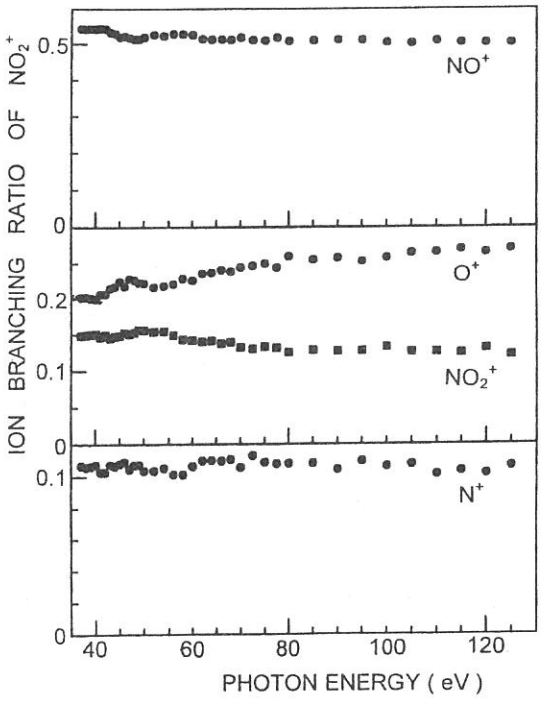

FIG. 3. Ion branching ratios of single photoionization of NO_2.

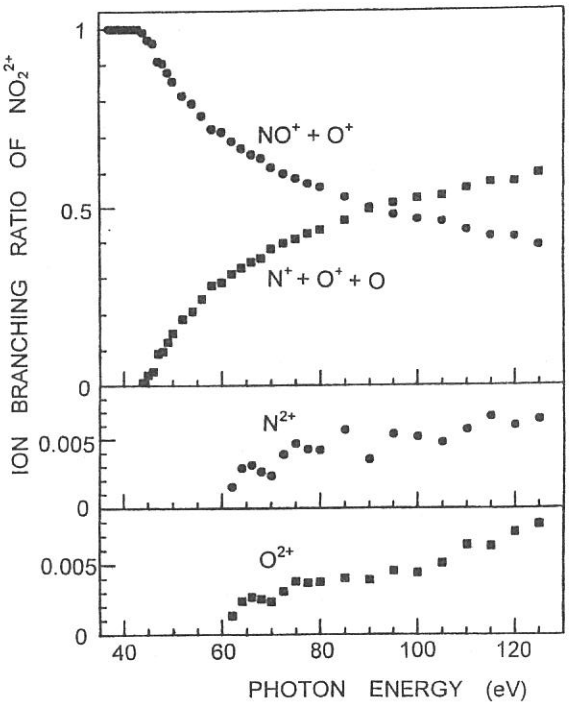

FIG. 4. Ion branching ratios of double photoionization of NO_2.

(BL3A2)

Laser Induced Fluorescence Excitation Spectroscopy of CN($X\ ^2\Sigma^+$, v = 0) Produced by VUV Photoexcitation of CH_3CN

Masakazu MIZUTANI, Hiromichi NIIKURA[A] and Koichiro MITSUKE

Department of Vacuum UV Photoscience, Institute for Molecular Science, Okazaki 444-8585, Japan
[A]The Graduate University for Advanced Studies, Okazaki 444-8585, Japan

It is important to measure the internal distribution of neutral fragments resulting from VUV photoexcitation of gas phase molecules because the internal distribution contains information on predissociation dynamics of superexcited states. However, detection of neutral fragments is difficult by means of conventional methods such as mass spectrometry and photoelectron spectroscopy. Unless the fragments experience radiative transition, fluorescence spectroscopy is ineffective.

The pump-probe experiment combining synchrotron radiation and a laser is expected to be one of the most effective method for probing ionic and neutral fragments resulting from VUV photoexcitation. We have developed laser induced fluorescence (LIF) excitation spectroscopy of ions prepared by VUV photoexcitation with synchrotron radiation. The rotational states of N_2^+($X\ ^2\Sigma^+$, v = 0) produced from N_2 or N_2O are resolved and their distribution is analyzed.[1-3] Following these experiments, we are trying to realize LIF excitation spectroscopy of neutral fragments produced by VUV photoexcitation.

A molecular beam of the sample gas of CH_3CN is expanded from a multi-capillary nozzle and subjected to photoexcitation with an intense undulator radiation (E_{SR} = 18 eV) which is supplied as the zeroth order light of a grazing-incidence monochromator. Formed neutral fragments, CN($X\ ^2\Sigma^+$, v''=0), are excited to the $B\ ^2\Sigma^+$, v'=0 state by irradiation of the second harmonic of a mode-locked Ti:sapphire laser. The fluorescence due to the transition ($B\ ^2\Sigma^+$, v'=0) → ($X\ ^2\Sigma^+$, v''=1) is detected by using a combination of an input optics, a secondary monochromator and a photon-counting system including a photomultiplier. As far as we know, there is no experimental work on laser spectroscopy of the CN($X\ ^2\Sigma^+$) radicals produced by VUV photoexcitation of CH_3CN. The signal intensity is estimated to be very low because the cross section for the formation of CN($X\ ^2\Sigma^+$) is no more than 1 Mb.

In order to improve the collection efficiency of the fluorescence, we are planning to improve the input optics. The revised optics consists of spheroidal and spherical mirrors and a optical fiber.

References

1) M. Mizutani, H. Niikura, A. Hiraya and K. Mitsuke, *J. Synchrotron Rad.* **5** (1998) 1069-1071.
2) K. Mitsuke, M. Mizutani, H. Niikura and K. Iwasaki, *Rev. Laser Eng.* **27** (1998) 458-462.
3) H. Niikura, M. Mizutani and K. Mitsuke, *Chem. Phys. Lett. in press.*

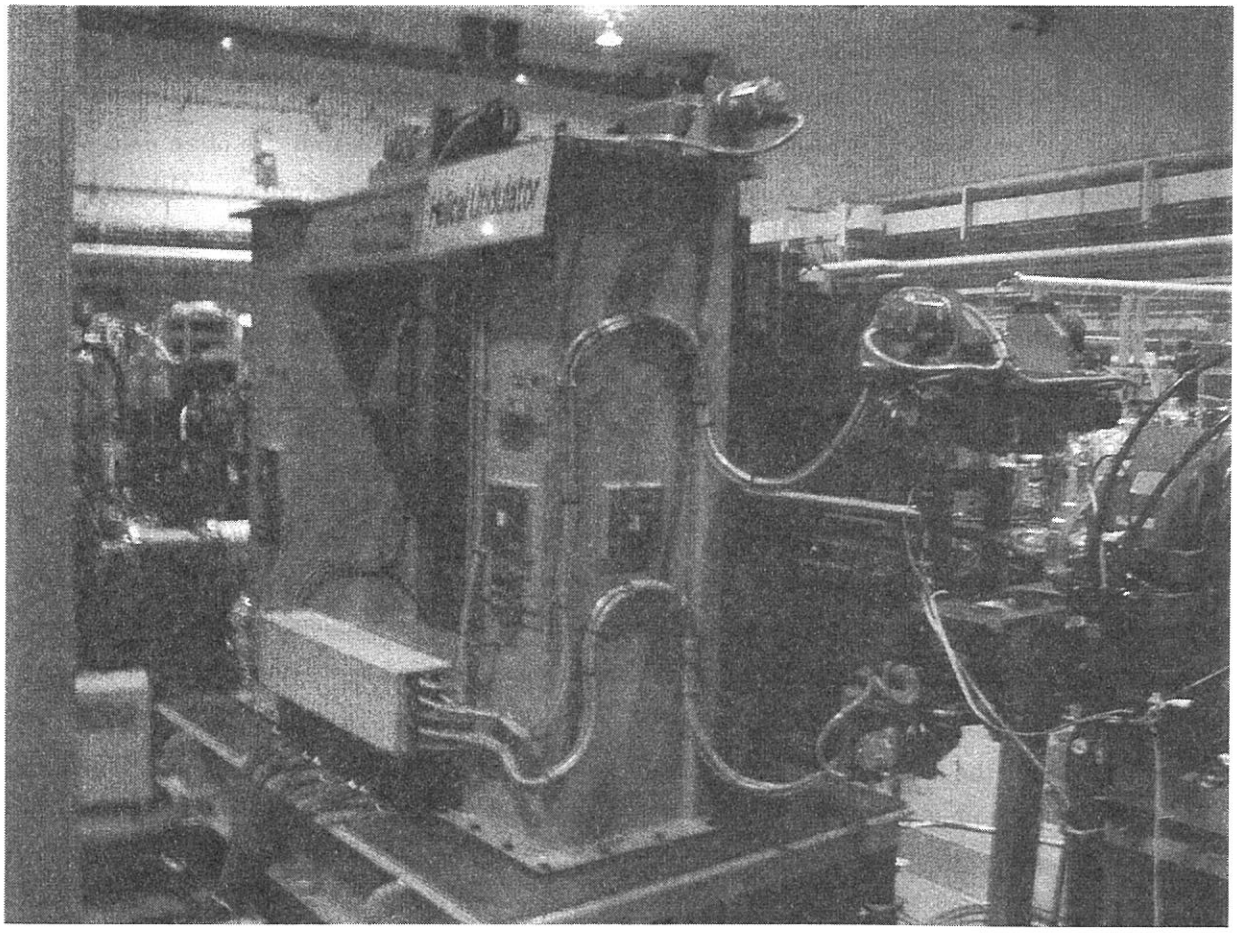

Helical Undulator

(BL3A2)

Fragmentation of $Cl_3SiC{\equiv}CSi(CH_3)_3$ vapor following Si:2*p* core-level photoexcitation. A search for a site-specific process in complex molecules

Shin-ichi Nagaoka and Joji Ohshita[A]

Institute for Molecular Science, Okazaki 444-8585 and [A]Department of Applied Chemistry, Faculty of Engineering, Hiroshima University, Higashi-Hiroshima 739-8527

Synchrotron radiation has provided a powerful means to obtain information about core-level excitations, and the dynamic processes following the core-level excitations in molecules have long been a subject of interest. In contrast to valence electrons that are often delocalized over the entire molecule, the core electrons are localized near the atom of origin. Although core electrons do not participate in the chemical bonding, the energy of an atomic core-level in the molecule depends on the chemical environment around the atom. A shift in the energy levels of core electrons that is due to a specific chemical environment is called a chemical shift.

Monochromatized synchrotron radiation can excite core electrons of an atom in a specific chemical environment selectively, discriminating the core electrons from those of like atoms having different chemical environments. This site-specific excitation often results in site-specific fragmentation, which is of importance in understanding localization phenomena in chemical reactions and which is potentially useful for synthesizing materials through selective bond breaking. Studies of the site-specific fragmentation of organosilicon molecules would also be of interest from the viewpoint of photochemical vapor deposition using synchrotron radiation in the processes of semiconductor fabrication.

To elucidate the site-specific fragmentation, we have studied the spectroscopy and dynamics following core-level photoionization of various molecules condensed on surfaces [1-4]. In contrast to the cases of $Cl_3SiSi(CH_3)_3$ and $F_3SiCH_2Si(CH_3)_3$, the site-specific fragmentation was clearly observed in the mass spectra of $F_3SiCH_2CH_2Si(CH_3)_3$ (FSMSE) in the vapor phase [2,3]; production of $SiCH_3^+$ and SiF^+ ions is enhanced by Si[Me]:2*p* and Si[F]:2*p* excitations, respectively. It is considered that the site-specific fragmentation is observed in molecules in which the two Si sites are located far apart and, thus, electron migration between the two Si-containing groups is not effective. In the present study, we studied the fragmentation of $Cl_3SiC{\equiv}CSi(CH_3)_3$ (CSMSA) vapor following Si:2*p* core-level photoexcitation to elucidate the effect of the unsaturated bond (C ≡C) between the two sites.

CSMSA was synthesized for the first time in this study with the reaction of $BrMgSiC{\equiv}CSi(CH_3)_3$ and $SiCl_4$. The experiments were performed using a time-of-flight spectrometer with variable path length, coupled to a constant-deviation grazing incidence monochromator installed on the BL3A2 beamline [5].

Figure 1 shows the total photoionization efficiency curve of CSMSA. Figure 2 shows an example of the photoionization mass spectrum of CSMSA taken in the photoelectron-photoion

coincidence (PEPICO) mode at a photon energy of 105 eV. Assignments are given in the figure. Figure 3 shows plots of the ratios of the integrated intensities of $SiCH_3^+$ and $SiCl^+$ peaks in the photoionization mass spectrum to the total photoion intensity ($I_{ion}/I_{tot\text{-}ion}$) as a function of photon energy. In contrast to the case of FSMSE, $I_{ion}/I_{tot\text{-}ion}$'s for $SiCH_3^+$ and $SiCl^+$ are similar to each other in CSMSA, except for the increase in the $I_{ion}/I_{tot\text{-}ion}$ for $SiCl^+$ at 110 eV. The site-specific fragmentation of CSMSA is less remarkable than that of FSMSA. Further investigations are clearly needed on the reason for this difference.

[1] S. Nagaoka, K. Mase, M. Nagasono, S. Tanaka, T. Urisu and J. Ohshita, J. Chem. Phys. 107, 10751 (1997).

[2] S. Nagaoka, T. Fujibuchi, J. Ohshita, M. Ishikawa and I. Koyano, Int. J. Mass Spectrom. Ion Processes 171, 95 (1997).

[3] S. Nagaoka, K. Mase and I. Koyano, Trends Chem. Phys. 6, 1 (1997).

[4] S. Nagaoka, K. Mase, M. Nagasono, S. Tanaka, T. Urisu, J. Ohshita and U. Nagashima, Chem. Phys. 249, 15 (1999).

[5] T. Masuoka and S. Nagaoka, Trends Chem. Phys. 3, 13 (1994).

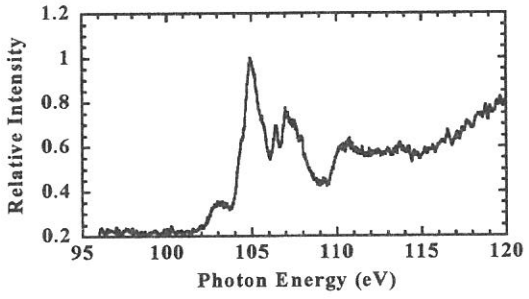

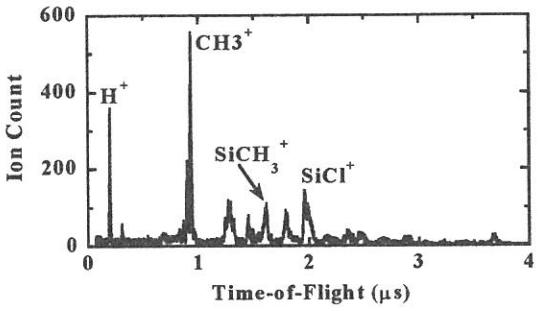

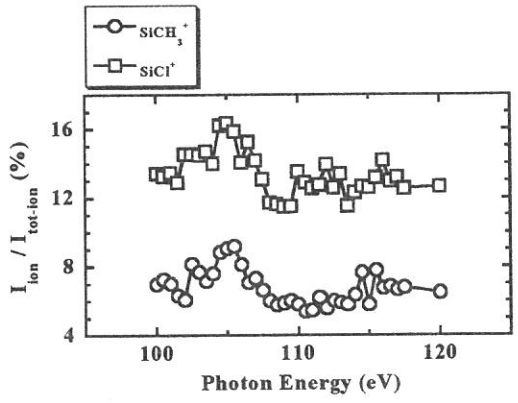

Figure 1 (upper left-hand side). Total photoionization efficiency curve of CSMSA. The slit widths of the monochromator were 0.2 mm, giving an optical resolution of 0.04 nm.

Figure 2 (upper right-hand side). Photoionization mass spectrum of CSMSA taken by excitation at 105 eV in the PEPICO mode. The slit widths of the monochromator were 0.2 mm, giving an optical resolution of 0.04 nm. Data collection time was 450 s.

Figure 3 (bottom). $I_{ion}/I_{tot\text{-}ion}$ for $SiCH_3^+$ and $SiCl^+$ in CSMSA as a function of photon energy. The slit widths of the monochromator were 0.2 mm, giving an optical resolution of 0.04 nm.

(BL3A2)

Rotational State Distribution of $N_2^+(X^2\Sigma_g^+, v = 0)$ formed by N_2O.

Hiromichi Niikura*, Masakazu Mizutani** and Koichiro Mitsuke**

*The Graduate University for Advanced Studies, ** Institute for Molecular Science,

Myodaiji, Okazaki, 444-8585, Japan.

The rotational temperature of $N_2^+(X\ ^2\Sigma_g^+, v = 0)$ formed by undulator radiation excitation of N_2O at 18.556 eV reduces to be 200 - 230 K from 300 K in the course of the dissociation [1]. Dissociation leading to $N_2^+(X\ ^2\Sigma_g^+) + O(^3P)$ is known to be promoted at E_{SR} = 18.556 eV by autoionization of the $3d\pi$ Rydberg state to the $N_2O^+(B^2\Pi)$ state. The energy released at a time of dissociation, referred to here as the *available* energy E_{avl}, are distributed to the fragment rotational energy in addition to the initial rotational energy of the parent $N_2O^+(B\ ^2\Pi)$, E_{avl} is defined by

$$E_{avl} = E_{SR} - E_{elec} - D_0 = I_E - D_0 \qquad (1)$$

where E_{SR} is the excitation photon energy for the $3d\pi$ Rydberg state (E_{SR} = 18.556 eV), D_0 is the NN-O bond dissociation energy (17.25 eV measured from the electronically ground state of N_2O), E_{elec} is the kinetic energy of the ejected electron, and I_E is the ionization energy for a vibrational state of N_2O^+ ($B\ ^2\Pi$).

The available energy is calculated from an Eq. 1 to be 3200 - 10500 cm^{-1} depending on I_E. On the other hand, the average rotational energy of the N_2^+ ($X\ ^2\Sigma_g^+$, v = 0) fragment is obtained from T = 220 K to be 150 cm^{-1}. The percentage of the rotational energy of $N_2^+(X\ ^2\Sigma_g^+, v = 0)$ to the available energy is thus only 1.5 - 5 %. This small fraction of the fragment rotational energy indicates that the available energy is distributed dominantly to the relative translational energies of N_2^+ and O and/or to the fragment vibrational energy.

The impulsive model assumes that the molecules dissociate so rapid that the available energy can not randomizes to the all phase space equally but is specified by the geometry at a instance of dissociation. The distribution of the available energy to the fragment rotational and/or vibrational energy of fragments are evaluated by using E_{avl}, the masses of the three atoms and the bond angle, θ ,of $N_2O^+(B\ ^2\Pi)$ in its equilibrium geometry. Unfortunately, the exact equilibrium geometry of N_2O^+ ($B\ ^2\Pi$) has not been elucidated yet because of a strong vibronic coupling between two electronic states located at around 17.5 eV whose configurations are expressed as $(2\pi)^{-2}$ $(3\pi)^1$ and $(1\pi)^{-1}$. It is possible that the ion with the former configuration has a bent equilibrium geometry on account of the accommodation of an electron in the π^* orbital. Therefore, we calculate the average rotational energy of $N_2^+(X\ ^2\Sigma_g^+, v = 0)$ as a function of θ by a similar procedure to that reported by *Levine* and *Valentini [2]* who have assumed a *stiff* NN bond and no vibrational excitation (*modified* impulsive model). For simplicity, we make further assumptions: The bond length of NN-O is equal to that of N-NO, the three atoms have the same mass, and the dissociation is assumed to proceed on the plane where the three atoms are located. The contribution of the bending motion to the fragment rotational energy is disregarded. A space-fixed Cartesian coordinate system is employed with the origin at the center of mass of N_2O^+. The rotational angular momentum of $N_2O^+(B\ ^2\Pi)$ perpendicular the molecular plane, namely, J_C, is taken as the initial angular momentum even in the C_s bent geometry.

Figure 1 shows the calculated rotational energy of $N_2^+(X\ ^2\Sigma_g^+, v = 0)$ as a function of θ when E_{avl} takes a value of 3200 cm^{-1}, assuming that the dissociation takes place from the vibrational ground state of $N_2O^+(B\ ^2\Pi)$, *i.e.*, at the lowest peak of the vibrational band (I_E = 17.65 eV) in the reported photoelectron spectrum. Two rotational energies were calculated which correspond to two extreme cases: the high J limit and low J limit. Those are classified by the direction between the initial rotation of $N_2O^+(B\ ^2\Pi)$ and the repulsive force generated at a time of dissociation. In the low J limit the calculated curve once goes down to zero and goes up again with decreasing bond angle. The increase in the rotational energy with decreasing bond angle is attributed to the increase in the component of the rotational angular momentum of $N_2^+(X\ ^2\Sigma_g^+, v = 0)$ resulting from the repulsive force. The dashed line at the rotational energy of 200 cm^{-1} shows the initial rotational energy of $N_2O^+(B\ ^2\Pi)$ at 300 K. The rotational energy of $N_2^+(X\ ^2\Sigma_g^+, v = 0)$ is smaller than that of the parent $N_2O^+(B\ ^2\Pi)$ at $\theta \geq 130°$ and $\theta \geq 165°$ in the low-J and high-J limits, respectively. This clearly suggests the possibility of less rotational excitation in $N_2^+(X\ ^2\Sigma_g^+, v = 0)$ than in $N_2O^+(B\ ^2\Pi)$ at $\theta \geq 130°$. The LIF spectrum of $N_2^+(X\ ^2\Sigma_g^+, v = 0)$ has demonstrated that the average rotational energy of $N_2^+(X\ ^2\Sigma_g^+, v = 0)$ is smaller than that of $N_2O^+(B\ ^2\Pi)$. From these considerations, we can draw the conclusion that the equilibrium bond angle for the vibrational ground state of $N_2O^+(B\ ^2\Pi)$ is larger than ~ 130°.

References

[1] H. Niikura, M. Mizutani and K. Mitsuke, Chem. Phys. Letters, 317 (2000) 45.

[2] H. B. Levene and J. J. Valentini, J. Chem. Phys., 87 (1987) 2594.

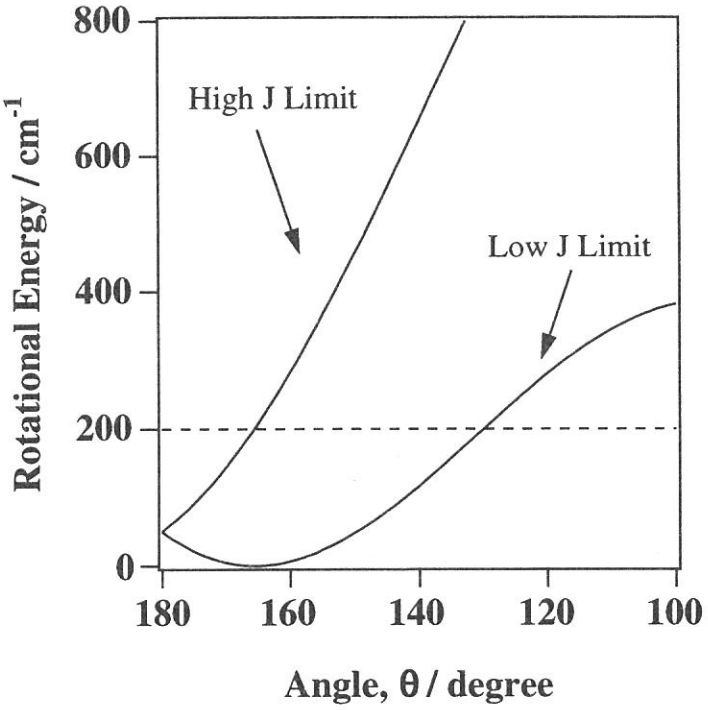

Figure 1. Calculated rotational energies of the N_2^+ fragment as a function of the bond angle θ on the basis of the modified impulsive model. Two rotational energies were calculated which correspond to the high J and low J limit (see text). The dashed line at the rotational energy of 200 cm^{-1} shows the initial rotational energy of N_2O^+ at 300 K.

(BL-3B)

Development of a new angle-resolved energy analyzer for photoelectron spectroscopy of polarized atoms

Kota IWASAKI and Koichiro MITSUKE

A Institute for Molecular Science, Myodaiji, Okazaki 444-8585 , Japan

A new angle-resolved electron energy analyzer incorporating a position sensitive detector (PSD) has been designed to measure the angular distribution of photoelectron from polarized rare gas atoms in BL3B. There are two ways to obtain the angular distribution of photoelectrons: rotating an energy analyzer with respect to its the symmetric axis or using angle-resolved energy analyzer. The former is simpler than the latter one, however the latter one gives promise of achieving good angular resolution and wide angular acceptance simultaneously. We think that an angle-resolved analyzer is needed to measure complicated angular distributions of photoelectrons caused by the atomic alignment with relatively short accumulation time of signals.

The following specifications are required for developing the analyzer available in the present experiment.

1. Photoelectrons should be detected with relatively good energy resolution that is smaller than the energy difference 177meV between $Ar^+(^3P_{1/2})$ and $Ar^+(^3P_{3/2})$. Since the energy resolution is generally proportional to the transmission energy, high resolution can be obtained in an analyzer of low transmission energy. However, we should consider the fact that transmission efficiency of an analyzer decreases as the transmission energy is reduced. The transmission energy is therefore expected to be larger than 3eV.

2. In our experiment, target atoms are excited with linearly polarized synchrotron radiation (SR) and ionized with YAG laser (532nm). Both two light beams intersect each other in the right angle, and the YAG laser beam is introduced to pass through an entrance slit and an exit hole of the electron analyzer. The exit hole should be designed to avoid the scattering of the laser light. Therefore, the width of the slit, defining the energy resolution, is determined from the diameter of the laser beam (ϕ2mm).

3. Angular resolution of a spherical analyzer equipped now in the end station of BL3B is about 8 degrees; this value is equal to the angular acceptance and not enough for our purpose. We intend to achieve better angular resolution and wider angular acceptance.

Considering these factors, we have newly designed a conical analyzer consisting of a set of an inner and outer conical deflector electrode, cylindrical lenses, a gas cell and a PSD unit as shown in Figure 1. Photoelectrons emitted in the gas cell are accelerate between the cell and an extractor electrode, then focused on an entrance slit by the cylindrical lenses. The trajectories of electrons between the inner and the outer conical electrodes are similar to those expected for a conventional parallel-plate analyzer. However, the conical analyzer

has rather larger energy dispersion and larger angular aberration than the parallel-plate analyzer. Energy selected electrons ejected from the conical deflector electrodes are detected with the PSD mounted behind the analyzer which consists of a resistive anode encoder of an effective diameter 40mm and micro-channel plates. The energy resolution is expressed as

$$\frac{\Delta E}{E} = \frac{\Delta R}{1.11R} + k_1\alpha + k_2\alpha^2 \approx \frac{1}{30},$$

where R denotes the distance between the entrance and exit slits, α the angular deviation of electrons about the mean trajectory of the incident electrons in the dispersion plane, and k_1 and k_2 angular aberration coefficients. On the other hand, the conical analyzer is incapable of focussing in the azimuth direction. The azimuth angular resolution is thus determined from the diameter of the sample volume (ϕ1mm) and the position sensitivity of PSD, and we expect the resolution of 1.5 degree. With fixing the PSD at certain position, the angular distribution can be measured in the range of 25 degrees at once. By rotating PSD about the synchrotron radiation propagation axis, we can obtain the photoelectron angular distribution from –5 to 95 degrees with respect to the electric vector of SR.

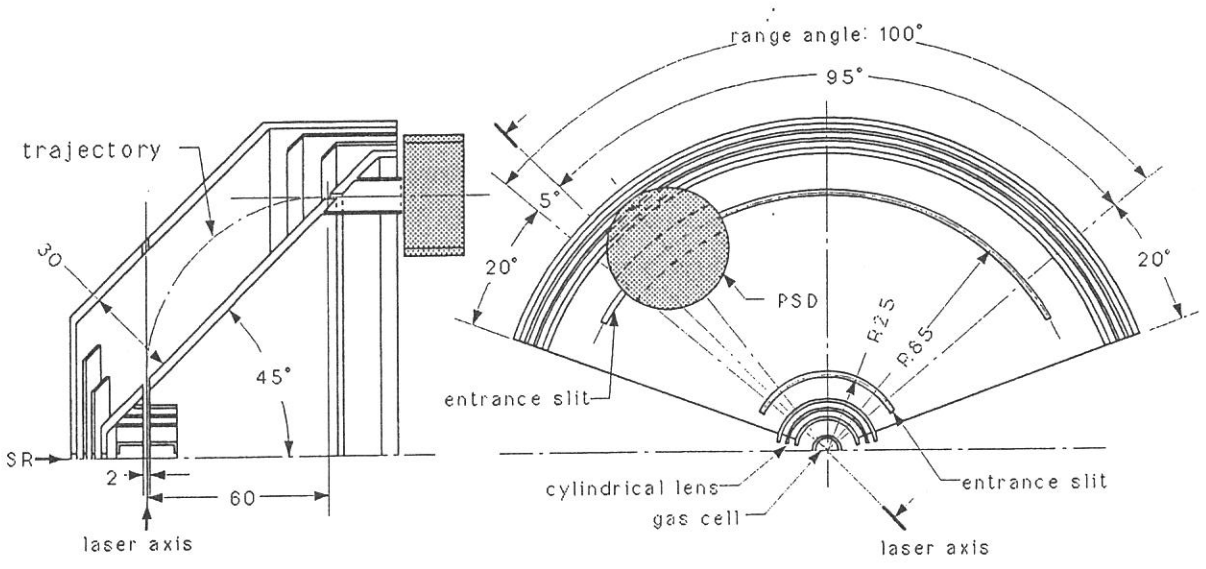

Figure 1. Schematic diagram of the conical analyzer. The principal electrodes of the analyzer are depicted by taking a cross sectional view on the plane which includes the propagation vectors of the laser and SR (left), and by taking a top view (right).

(BL8B1)

Site-selective fragmentation of core-excited acetylacetone

Hiroaki YOSHIDA, Takatoshi YANAGIHARA , Takashi TOKUSHIMA, Yasunori SENBA,

Katsutoshi SHIRASAWA, Katsura KAMIMORI, Atsunari HIRAYA

Department of Physical Sciences, Hiroshima University, Kagamiyama, Higashi-Hiroshima

739-8526, Japan

Site-selective fragmentation of acetylacetone ($CH_3COCH_2COCH_3$) after an excitation of oxygen 1s electron has been studied. Ion yields of m/e=15 (CH_3^+) and 43 (CH_3CO^+) obviously increase at an oxygen 1s→π^* excitation by comparing pre-edge excitation. On the other hand, ion yield of only m/e=15 (CH_3^+) shows a prominent enhancement at an oxygen 1s ionization region. Precursor states of these fragmentation processes are discussed from a viewpoint of resonant and normal Auger decay processes.

Experiments were carried out at BL8B1 of UVSOR. Synchrotron radiation from bending magnet is dispersed by a constant-length-type spherical-grating monochromator. Energy resolution (E/ΔE) of the monochromator is set to about 500 at 500eV. Produced ions are detected by a reflectron-type time-of-flight mass spectrometer. Mass resolution (m/Δm) is about 600 for zero-energy ions.

Total ion yield curve in the oxygen K-edge region in Fig.1 shows a remarkable peak structure at 531.4eV. By comparing the peak position to that of acetone $(CH_3)_2CO$, 530.4eV, the peak is assigned to O1s→$\pi^*_{C=O}$ resonance. A broad structure above about 540eV is ascribed to transitions to the ionization continuum of oxygen 1s electron. Mass spectra were obtained at the energy of a) pre-edge, b) π^*, and c) ionization continuum (Icont) excitations. Contributions by pre-edge excitation were subtracted from raw spectra for π^* and Icont in Fig.2. Ion yields of the specific mass number such as m/e=15 (CH_3^+) and 43(CH_3CO^+) obviously increase at an oxygen 1s→$\pi^*_{C=O}$ excitation by comparing pre-edge. Resonant Auger decay around C=O, which produces a single-charged ion, would weaken the strength of either C-C bond neighboring C=O as shown below.

i) $H_3C\text{-}C{=}O^*\text{-}CH_2COCH_3 \rightarrow H_3C^+\text{—}C{=}O\text{-}CH_2COCH_3 \rightarrow H_3C^+\text{-} \quad \text{-}C{=}O\text{-}CH_2COCH_3$

ii) $H_3C\text{-}C{=}O^*\text{-}CH_2COCH_3 \rightarrow H_3C\text{-}C^+{=}O\text{—}CH_2COCH_3 \rightarrow H_3C\text{-}C^+{=}O\text{-} \quad \text{-}CH_2COCH_3$

CH_3^+ and CH_3CO^+ are, thus, produced effectively after an excitation of oxygen 1s electron to $\pi^*_{C=O}$ orbital. On the other hand, only m/e=15 (CH_3^+) ion yield prominently enhanced at an

oxygen 1s ionization region. Normal Auger decay around C=O, which produces a double-charged ion, would weaken the strength of both C-C bonds neighboring C=O as shown below.

iii) $H_3C\text{-}C{=}O^+\text{-}CH_2COCH_3 \rightarrow H_3C^+—C{=}O—{}^+CH_2COCH_3$

$\rightarrow H_3C^+\text{-} \quad C{=}O \quad \text{-}{}^+CH_2COCH_3$

Coulomb explosion caused by a hole-hole repulsion initially makes ion pairs of CH_3^+ and $CH_2COCH_3^+$. The fact that m/e=57 ($CH_2COCH_3^+$) is not observed in the mass spectra suggests the sequential dissociation of $CH_2COCH_3^+$ into various kinds of fragments. As a result, only CH_3^+ is produced effectively after an ionization of oxygen 1s electron.

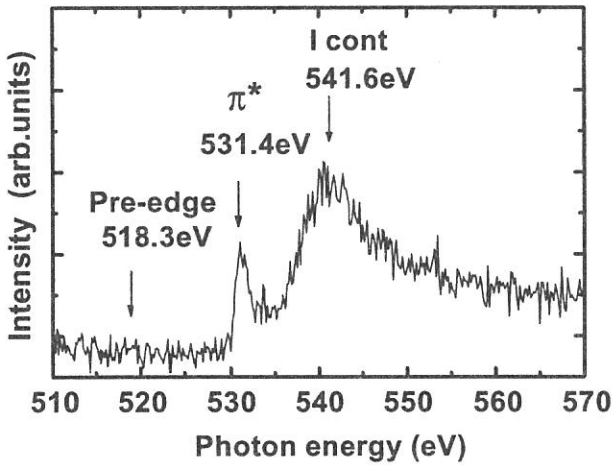

Fig.1 Total ion yield of acetylacetone in the oxygen K-edge region.

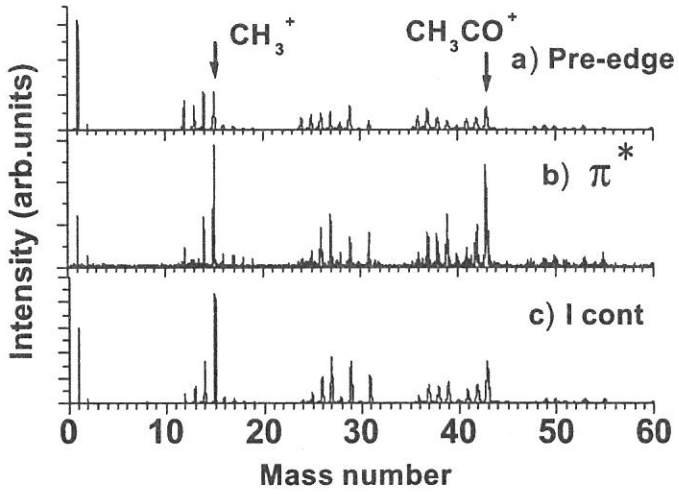

Fig.2 Mass spectra of acetylacetone following a) pre-edge, b) O1s→π*, and c) O1s→ ionization continuum (Icont) excitations. Contributions by pre-edge excitation were subtracted from raw spectra for π* and Icont.

(BL8B1)

The measurement of PEPICO spectra at BL8B1 with photoelectron energies being selected

Tatsuo Gejo, Kazuhiko Mase, Shin-ichiro Tanaka, Shin-ichi Nagaoka
Eiji Ikenaga[A] and Iwao Shimoyama[B]
Institute for Molecular Science, Myodaiji, Okazaki 444-8585, Japan
[A]Faculty of Science, Hiroshima Uviv., Higashi-Hiroshima 739, Japan
[B]Faculty of Science, Kobe Univ., Kobe 657-8501, Japan

Fragmentation and ionization process of inner-shell excited molecules has been investigated by the excitation with synchrotron radiation. When one measures time-of-flight (TOF) spectra of ionic fragments generated from these core-ionized molecule, selecting the energy of the double charged ion energy by photoelectron analyzer allows us to select a defined initial state. This measurement is called PEPICO (photoelectron-phootion-coincidence) or AEPICO (Auger electron-photoion-coincidence) spectroscopy.

A CMA type electron energy analyzer with a TOF apparatus has been constructed and installed at beamline 8B1 in UVSOR for the measurement of the PEPICO spectra. TOF spectra have been observed with photoelectron energies being selected by this analyzer. In order to evaluate this analyzer we used soft X-ray of synchrotron radiation as a photon source and N_2 and CO_2 as target molecules.

Fig. 1 shows the 2D image of PEPICO spectra, in which the TOF spectra was shown with selecting a given photoelectron kinetic energy. The peak around 420 ns can be attributed to the N^+ and those around 650 ns arise from N_2^+. In this figure, strong correlation between Auger electron around 390 eV and the generation of N_2^+ has been observed, suggesting that N_2^+ are mainly generated via $3\sigma_g^{-1}$ Auger decay process. With this technique, we will try the triple coincidence of ionic fragments of molecules.

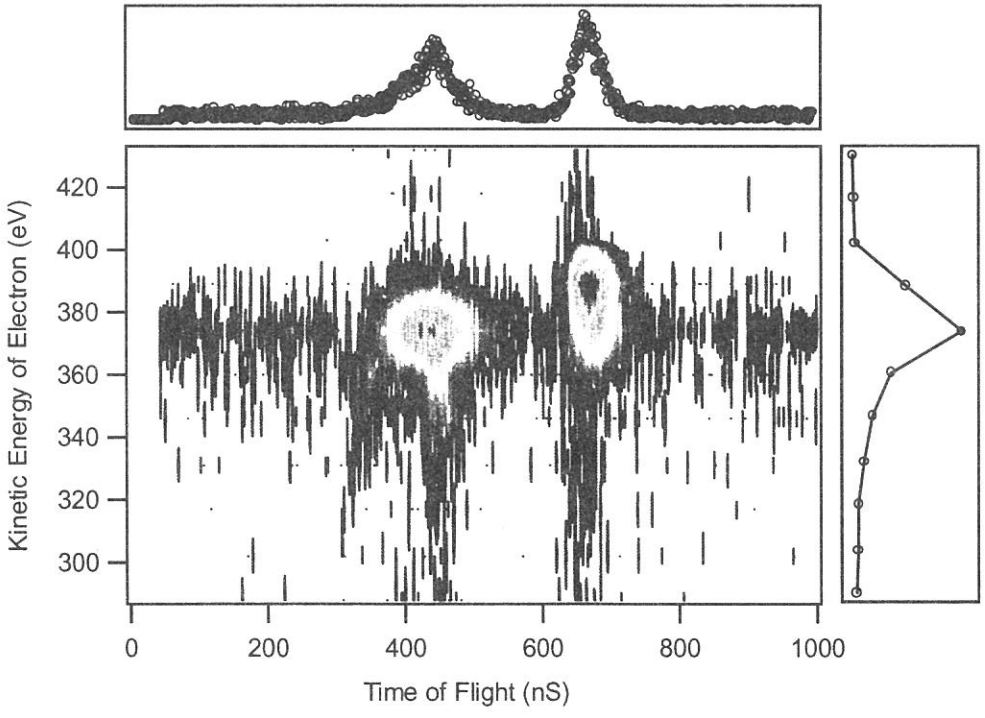

Fig. 1: PEPICO spectra of N_2.